Supporting Information

Sb_2O_3 Nanoparticles Anchored on Graphene Sheets via Alcohol Dissolution-Reprecipitation Method for Excellent Lithium Storage Properties

Xiaozhong Zhou, [a,*] *Zhengfeng Zhang,*[a] *Xiaofang Lu,*[a] *Xueyan Lv,*[a] *Guofu Ma,*[a] *Qingtao Wang,* [a] *Ziqiang Lei*[a,*]

[a] Key Laboratory of Eco-Environment-Related Polymer Materials of Ministry of Education, Key Laboratory of Polymer Materials of Gansu Province, College of Chemistry and Chemical Engineering, Northwest Normal University, Lanzhou 730070, Gansu Province, P.R. China.

[*] **Corresponding Authors**

Xiaozhong Zhou, E-mail: zxz20004@163.com, Tel/Fax: +86 931 7972663

Ziqiang Lei, E-mail: leizq@nwnu.edu.cn, Tel/Fax: +86 931 7971261

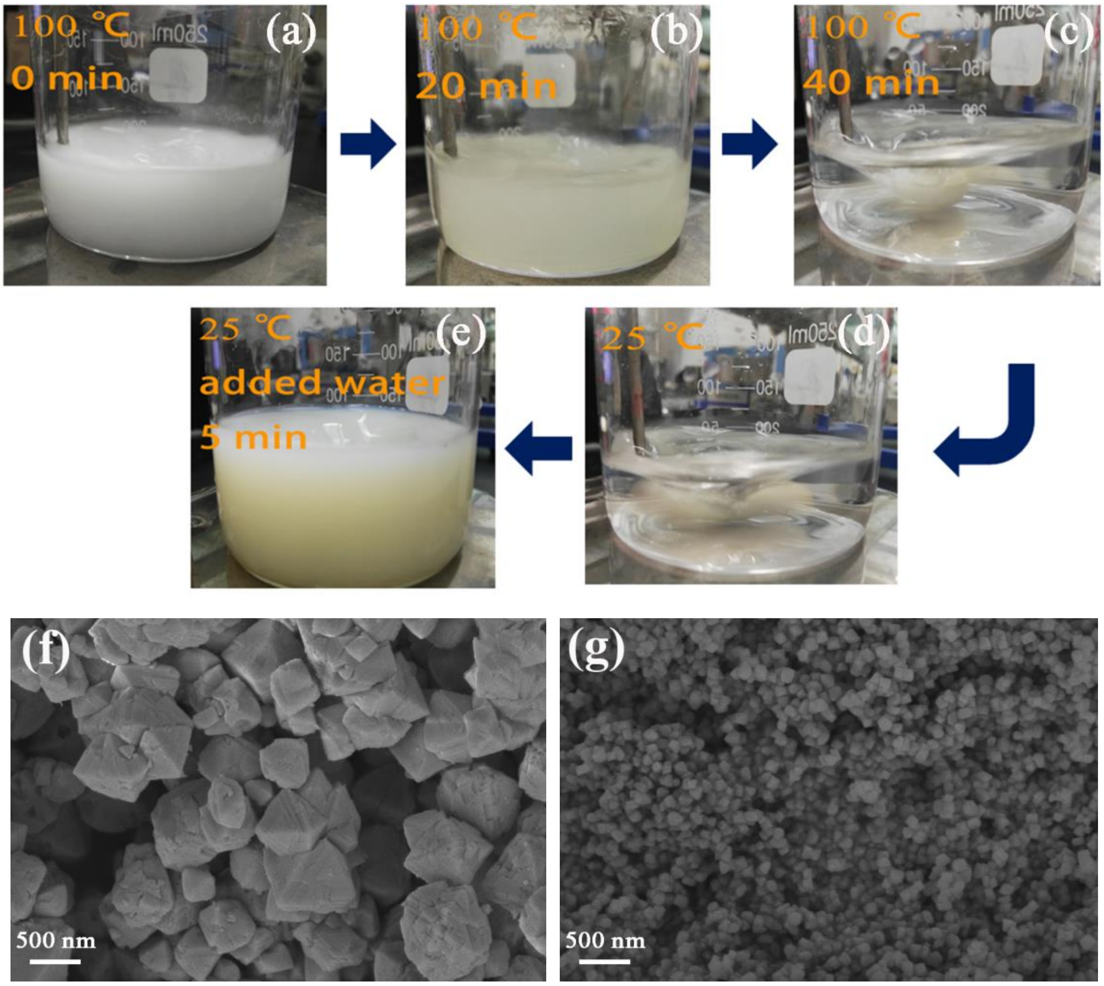

Figure S1 Digital camera images for the procedure of dissolution and reprecipitation of Sb_2O_3 in ethylene glycol (EG) solution. Sb_2O_3 particles were dispersed by magnetic stirring at 100 ^oC to form a milk white suspension (a). As continuous stirring, the suspension gradually became transparent (b and c), due to the formation of ethylene glycol antimony (EG-Sb). After cooling to 25 ^oC, the solution maintained transparent on account of good chemical stability (d). The EG-Sb was hydrolyzed with addition of water and the Sb_2O_3 was reprecipitation (e). SEM images for bulk Sb_2O_3 obtained in its initial condition (f) and after the procedure of dissolution and reprecipitation in EG solution (g).

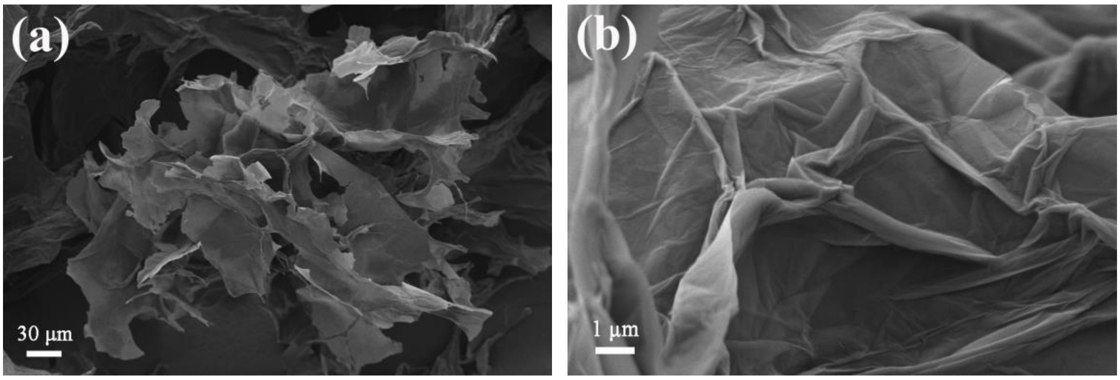

Figure S2 SEM images with low (a) and high (b) magnification of the as-prepared GO.

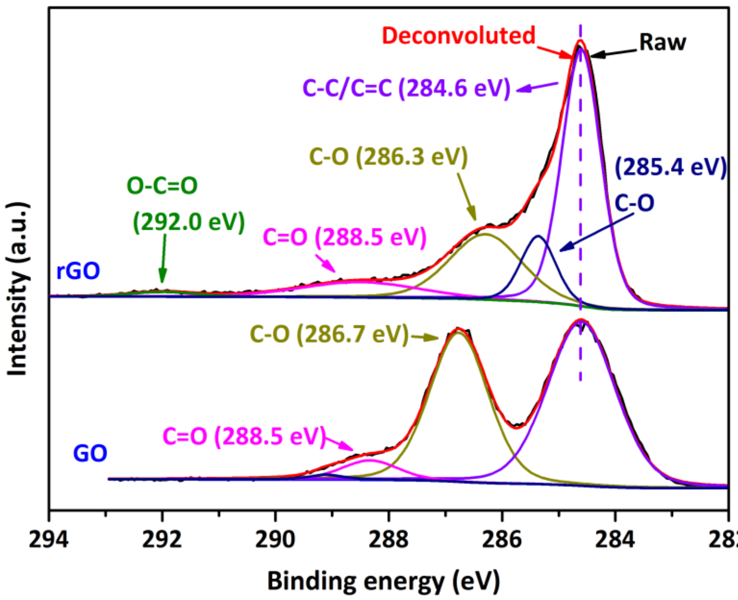

Figure S3 High-resolution C1s XPS spectra of GO and rGO samples.

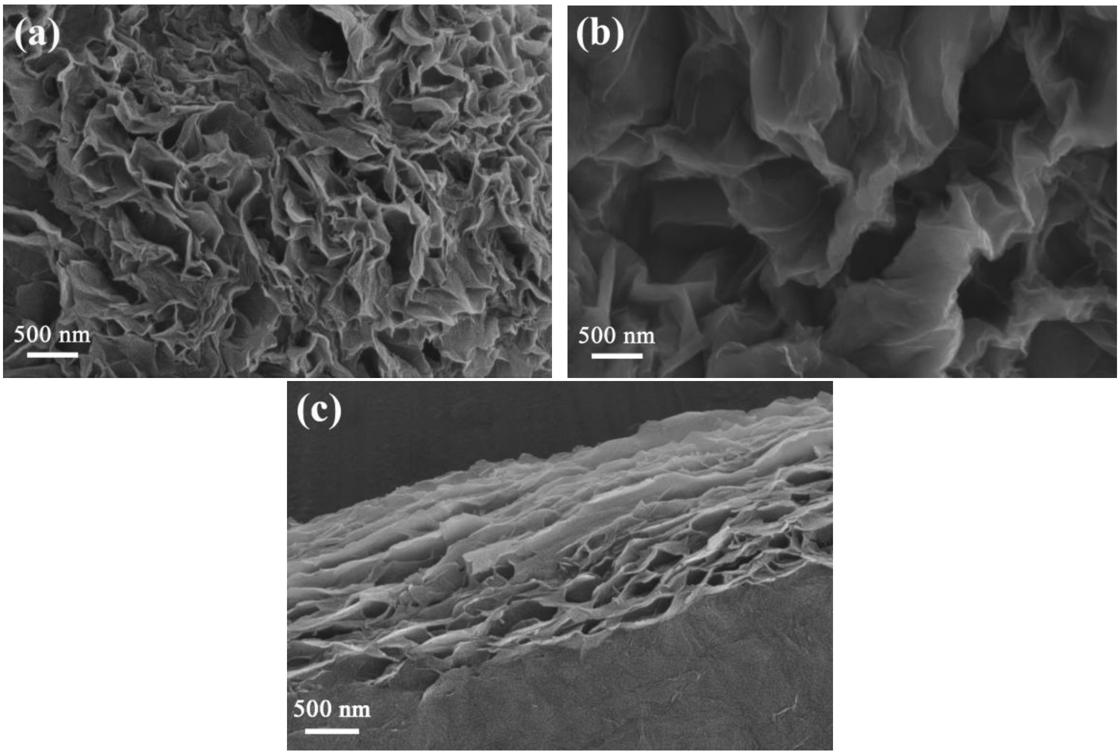

Figure S4 SEM images for rGO obtained without the addition of L-AA (a), with a 24-hour stirring at room temperature before (b) and after (c) solvothermal treatment.

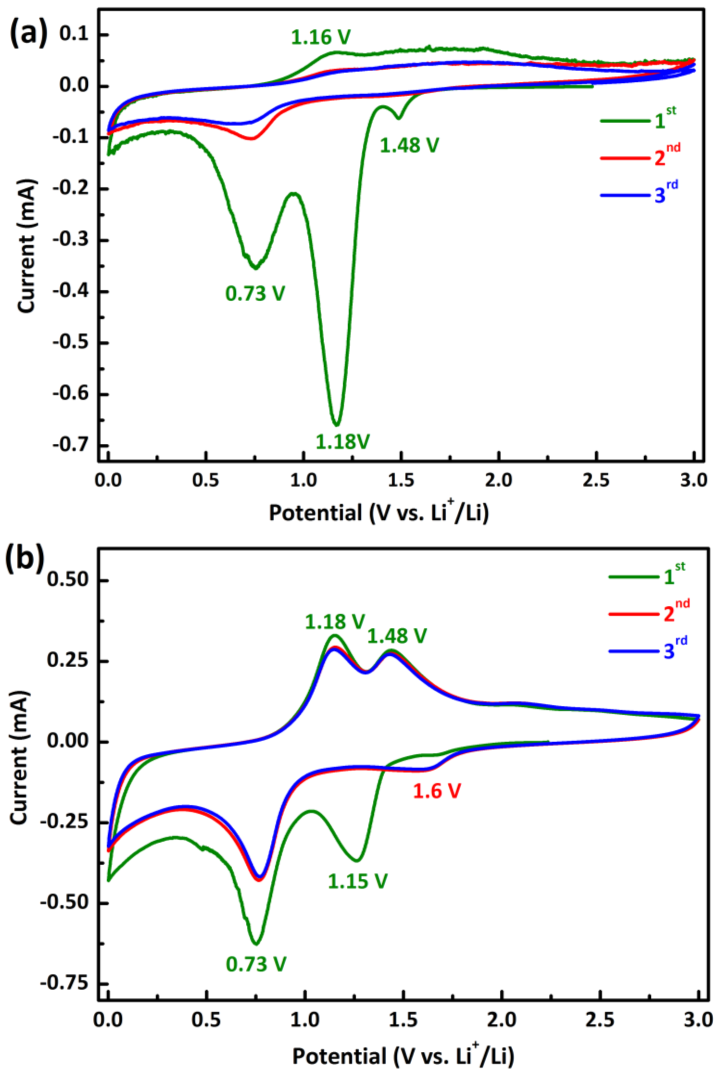

Figure S5 Cyclic voltammograms of initial three cycles for bulk Sb_2O_3 (a) and Sb_2O_3-rGO (b) eletrodes at a scan rate of 0.2 mV s^{-1}

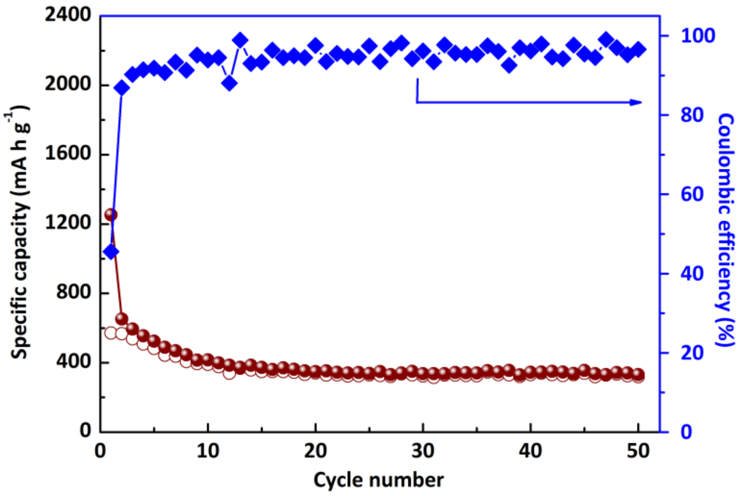

Figure S6 Cycling performance (left *y*-axis) and Coulombic efficiencies (right *y*-axis) of the bare rGO electrode at 100 mA g^{-1}

Table S1. Summary of the Sb_xO_y based electrodes materials for LIB applications.

Materials	Initial reversible capacity (mAh g^{-1} /A g^{-1})	ICE (%)	Capacity after (x) cycles (mAh g^{-1} / cycles)	Capacity at high rate (mAh g^{-1} /A g^{-1})	Long-term cycling capacity after (x) cycles (mAh g^{-1} / A g^{-1} / cycles)	Potential (V)	Ref.
Sb_2O_3 thin films	794 / -	77.2	~750 / 70	-	-	0.01-3	1
Sb_2O_3/rGO	899 / 0.05	50.8	562 / 100	155 / 0.3	-	0.01-3	2
Sb_6O_{13}/rGO	1271 / 0.1	45.8	1109 / 140	201 / 3	430 / 0.5 / 300	0.01-3	3
Sb_2O_4/rGO	1170 / 0.1	53.8	798 / 200	320 / 3	428 / 0.55 / 500	0.01-3	4
hollow Sb_2O_4	727.1 / 0.1	67.1	700 / 50	370.9 / 2	415 / 1 / 100	0.01-3	5
Sb_2O_3/rGO	1355 / 0.1	60	808 / 120	188 / 5	525 / 0.6 / 700	0.001-3	This work

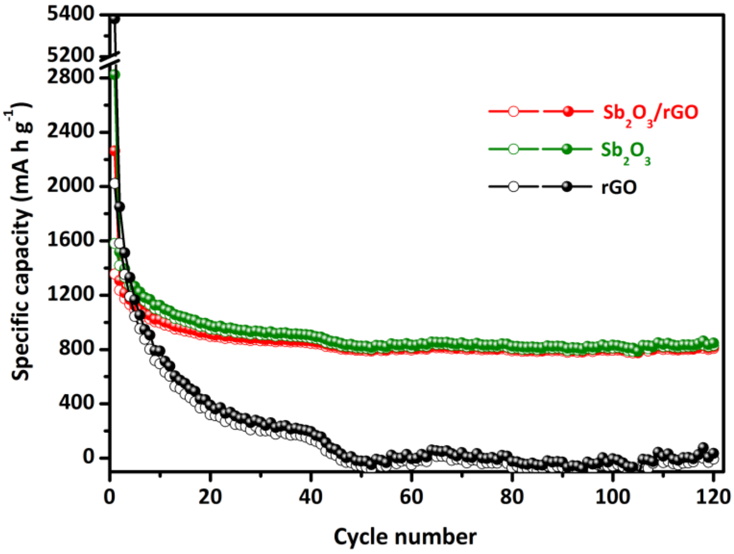

Figure S7 Capacity contribution from Sb_2O_3 or rGO during cycling in the Sb_2O_3/rGO nanocomposite, hypothesizing rGO contributed the fixed theoretical capacity of 744 mA h g^{-1} or Sb_2O_3 contributed the fixed theoretical capacity of 1109 mA h g^{-1} during cycling, respectively.

REFERENCES

(1) Xue, M.-Z.; Fu, Z.-W. Electrochemical Reaction of Lithium with Nanostructured Thin Film of Antimony Trioxide. *Electrochem. Commun.* **2006**, *8*, 1250-1256.

(2) Zhou, J.; Zheng, C.; Wang, H.; Yang, J.; Hu, P.; Guo, L. 3D Nest-Shaped Sb_2O_3/RGO Composite Based High-Performance Lithium-Ion Batteries. *Nanoscale* **2016**, *8*, 17131-17135.

(3) Zhou, X.; Zhang, Z.; Xu, X.; Yan, J.; Ma, G.; Lei, Z. Anchoring Sb_6O_{13} Nanocrystals on Graphene Sheets for Enhanced Lithium Storage. *ACS Appl. Mater. Interfaces* **2016**, *8*, 35398-35406.

(4) Zhou, X.; Zhang, Z.; Wang, J.; Wang, Q.; Ma, G.; Lei, Z. Sb_2O_4/Reduced Graphene Oxide Composite as High-Performance Anode Material for Lithium Ion Batteries. *J. Alloys Compd.* **2017**, *699*, 611-618.

(5) Yi, Z.; Han, Q.; Li, X.; Wu, Y.; Cheng, Y.; Wang, L. Two-Step Oxidation of Bulk Sb to One-Dimensional Sb_2O_4 Submicron-Tubes as Advanced Anode Materials for Lithium-Ion and Sodium-Ion Batteries. *Chem. Eng. J.* **2017**, *315*, 101-107.